Evaluation of Single- and Dual-Wavelength Radar Rain Retrieval Algorithms

Liang Liao
GESTAR/MSU, Greenbelt, MD

Robert Meneghini
NASA/GSFC, Greenbelt, MD

Ali Tokay
UMBC/JCET, Greenbelt, MD

Introduction

An important goal of the GPM DPR is to derive rain rate by estimating parameters of the DSD that is often modeled by an analytical function. Several dual-wavelength radar retrieval techniques have recently been developed, some of which are based on the method that uses the difference of radar reflectivities between two wavelengths to first infer the DSD parameters, correct attenuation and then derive rain rate gate by gate either along radar beam (forward recursive approach) or in reverse direction (backward recursive approach). To improve robustness of the dual-wavelength retrieval for the GPM mission, a few optimal methods have recently been proposed in which one or more adjustment factors are used to modify some nominal relationships between radar and hydrometeor's parameters to account for DSD variation in space and time. Adjustment factors at each gate/profile are determined by optimizing predefined cost functions that tend to satisfy dual-wavelength reflectivities and measured PIAs.

Because of spatial and temporal variations in DSD and also because of the fact that retrieval problems are often under-constrained, none of these retrieval methods are perfect. Their accuracies depend on several factors that include DSD parameterization, vertical homogeneity of DSD profiles and accuracy of the PIA estimates as well as the nominal radar-hydrometeor relations used for retrieval. A physical evaluation of these techniques is necessary not only for understanding uncertainties in rain estimation but also in gaining insight into ways to improve the algorithms. An important validation procedure for satellite retrievals is to examine radar estimates against ground measurements, such as ground radar and rain gauge networks. As a result of geometrically sample differences in satellite and ground radar measurements as well as their temporal offsets, certain degree of intrinsic uncertainties exists in these validation processes. These, along with other unknown errors related to radar measurements, such as NUBF and radar calibrations, pose a serious challenge to physically evaluate the impacts of various model assumptions and constraints involved in the algorithms on their performances and to check the algorithm robustness to possible measurement errors. To circumvent these un-avoided uncertainties, we employ measured DSD in this study to investigate performance of radar rain estimates by comparing the radar and hydrometeor parameters retrieved with those directly derived from DSD measurements. The robustness of the algorithms with respect to SRT random errors and inhomogeneity of vertical DSD profiles are also studied. One important advantage of using DSD data in simulating radar and rain profiles is existence of the "true" radar reflectivities, rain rates and characteristic DSD parameters with which the algorithm retrieval errors are tractable with respect to changes in the model and constraint settings. To construct realistic hydrometeor profiles, the measured DSD data acquired from a variety of storm systems are used, including the multiple Parsivel[2] observations acquired during the Iowa Flooding Studies (IFloodS), the Integrated Precipitation Validation Experiment (IPHEx) and data from NASA Wallops Flight Facility in Wallops Island, Virginia as well as the Olympic Mountains Ground Validation Experiment (OLYMPEX) field campaign.

ACKNOWLEDGEMENTS: This work is supported by Dr. R. Kakar of NASA Headquarters under NASA's Precipitation Measurement Mission (PMM) Grant NNH12ZDA001N-PMM.

DSD Profiles

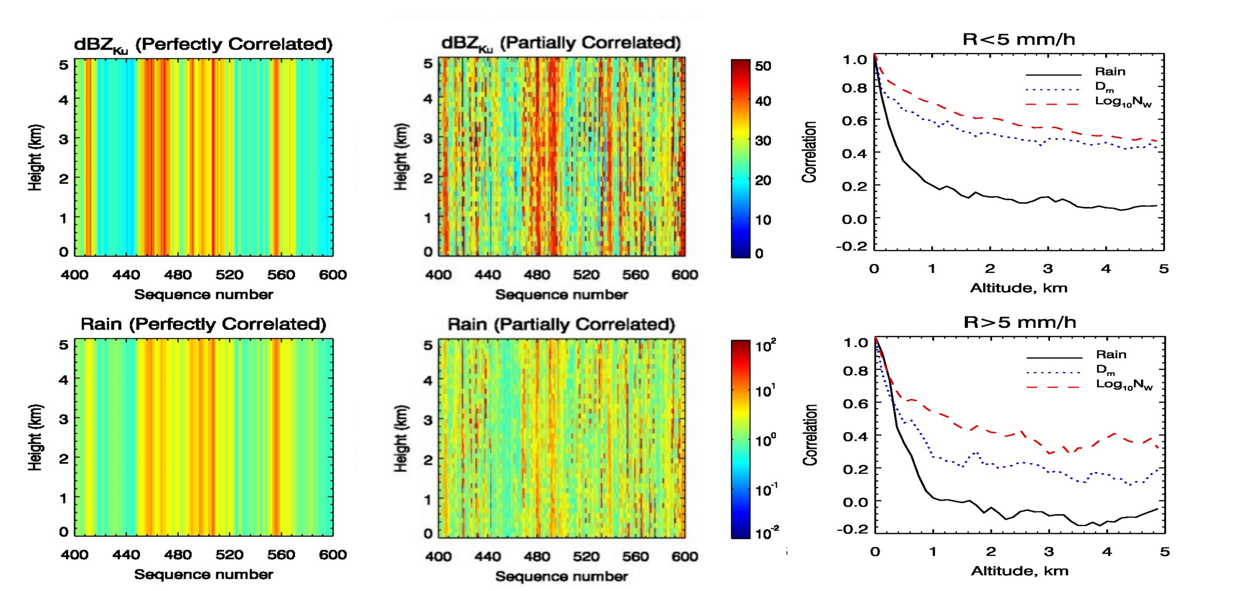

Fig.1 Examples of vertical DSD profiles (left and middle) and spatial correlation relative to surface rain (right).

DPR-Like Scheme

From R-D_m relation expressed as

$$R = \varepsilon^{\tau} a D_m^b \qquad (1)$$

From Look-up tables

$$R = N_w I_R(D_m,\mu) \qquad (2)$$

Then, we have

$$N_w = \frac{R}{I_R(D_m,\mu)} = \frac{\varepsilon_k^{\tau} a D_m^b}{I_R(D_m,\mu)} \qquad (3)$$

And also,

$$Z_e = 10\mathrm{Log}_{10}(N_w) + I_b(D_m,\mu)$$

Substituting (3) into above equation, we obtain

$$Z_e = 10\mathrm{Log}_{10}(\varepsilon_k^{\tau} a) + 10b\mathrm{Log}_{10}D_m - 10\mathrm{Log}_{10}I_R(D_m,\mu) + I_b(D_m,\mu) \qquad (4)$$

D_m could uniquely be solved from Eq.(4). Once D_m is determined, R and N_w are obtained from Eq.(1) and (3), respectively. From derived DSD parameters Z(λ) and k(λ) are then computed.

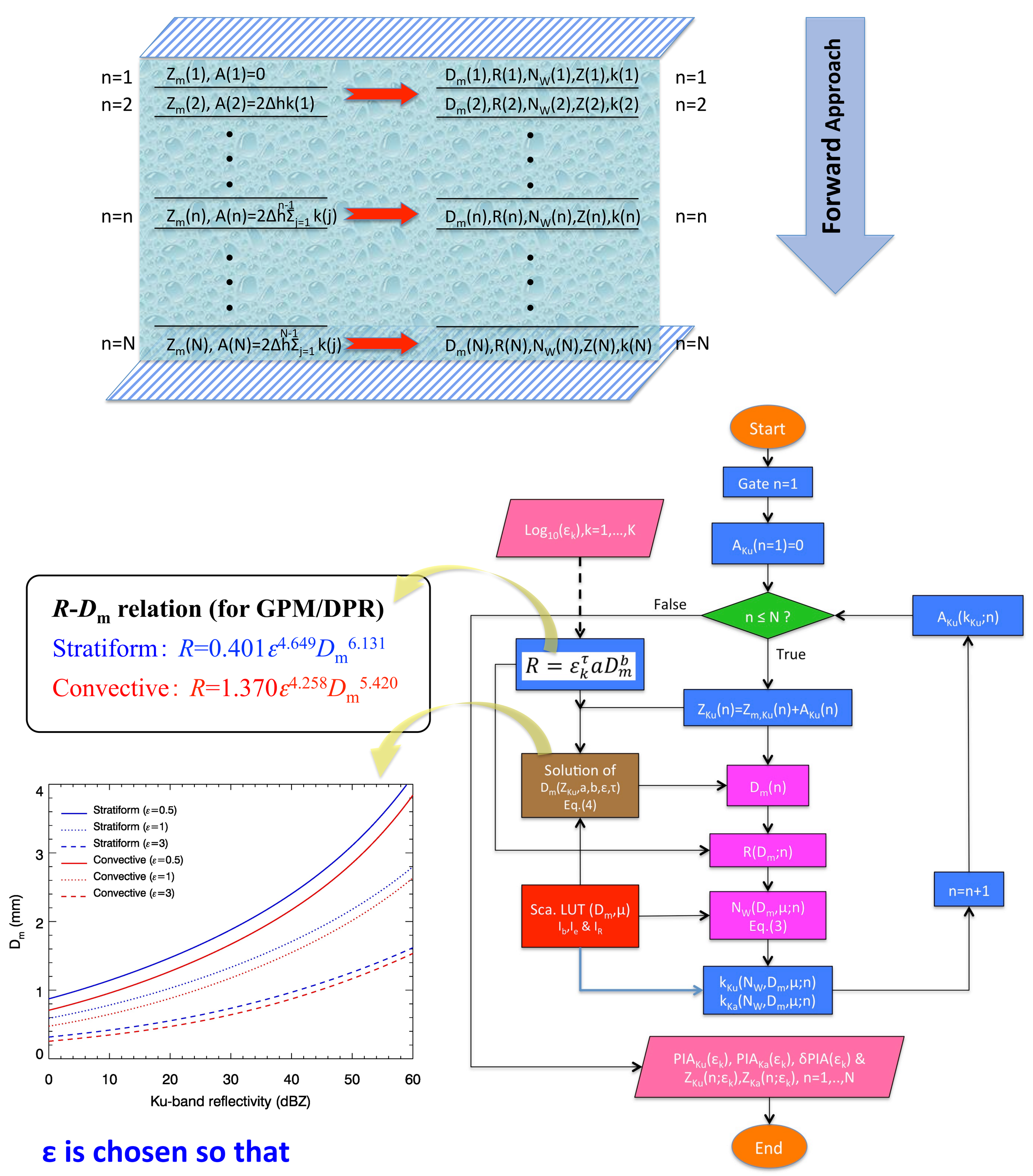

ε is chosen so that

$$p_1(\varepsilon)p_2(\varepsilon)p_3(\varepsilon) = \max\left(p_1(\varepsilon_k)p_2(\varepsilon_k)p_3(\varepsilon_k), k = 1,2,\ldots,K\right)$$

$$p_1(\varepsilon) = \frac{1}{\sigma_1\sqrt{2\pi}}\exp\left(-\frac{(\log\varepsilon)^2}{2\sigma_1^2}\right)$$

$$p_2(\varepsilon) = \frac{1}{\sqrt{2\pi}}\exp\left(-\frac{(\delta PIA - \delta PIA_{SRT})^2}{2\sigma_2^2}\right)$$

$$p_3(\varepsilon) = \prod_{l=1}^{N}\frac{1}{\sqrt{2\pi}}\exp\left(-\frac{(Z_{m,l,est}^{(Ka)} - Z_{m,l,pbs}^{(Ka)})^2}{2\sigma_3^2}\right)$$

Reference:

Seto, S., T. Iguchi and T. Oki, 2013: The basic performance of a precipitation retrieval algorithm for the Global Precipitation Measurement mission's single/dual frequency radar measurements. *IEEE Trans. Geosci. Remote Sens.*, **51**, 5239–5251.

Seto, S., and T. Iguchi, 2015: Intercomparison of attenuation correction methods for the GPM dual-frequency precipitation radar. *J. Atmos. Oceanic Technol.*, **32**, 915-926.

Dual-λ Techniques

1. Standard dual-wavelength technique

As DSD is parameterized as gamma distribution with its characteristic parameters N_W, D_m and μ, the differential frequency ratio (DFR), defined by

$$\mathrm{DFR} = 10\mathrm{Log}_{10}(Z_{Ku}/Z_{Ka}) = \mathrm{dBZ(Ku)} - \mathrm{dBZ(Ka)},$$

can be used to derive D_m when μ is assumed to be constant, e.g., μ=3 for TRMM PR and GPM DPR. An example of relationship between DFR and D_m computed from Pasivel DSD data, is shown in Fig.2.

Once D_m is obtained, N_W can be derived from either Z(Ku) or Z(Ka).

Although the standard dual-λ method is in principle fully accounts for spatial and temporal DSD variations and it is independent of empirical relations as some algorithms rely, its significant drawbacks are the double solutions of Dm when DFR<0 and small differences of DFR between Ku and Ka bands when D_m is roughly less than 1.5 mm as their measurements tend to move into Rayleigh region in which particle sizes matter most not wavelengths.

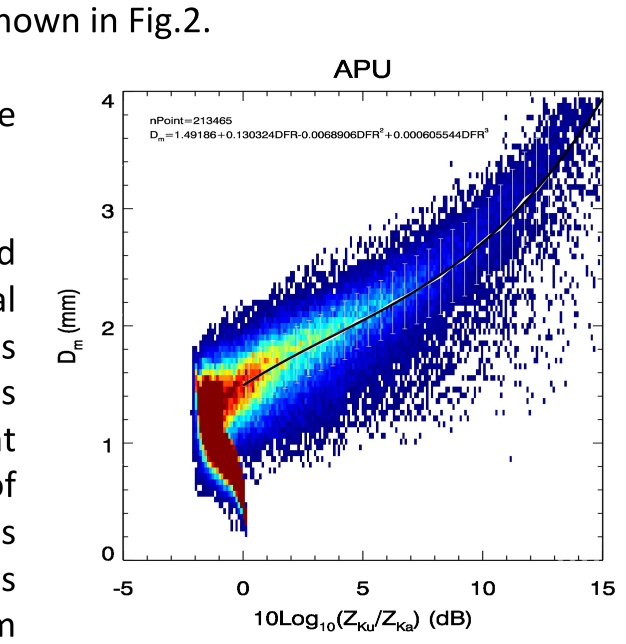

Fig.2 2-demensional PDF of Ku- and Ka-band DFR and D_m derived from the Parsivel disdrometer measurements during a few NASA ground validation field campaigns.

2. Modified DFR

To avoid double solutions of D_m from DFR-D_m relations as mentioned above, a modified version of DFR, denoted by DFR*, is introduced and defined by

$$\mathrm{DFR}^* = Z(\mathrm{Ku}) - \gamma Z(\mathrm{Ka}) \ \ (\mathrm{dB})$$

where γ is from 0 to 1. The modified DFR* defined in above equation is intended to partially use Ka-band measurements, with its extreme cases, i.e., γ=0 and 1, representing single Ku-band and standard dual-λ approaches, respectively. To illustrate how D_m is related to modified DFR*, Fig.3 depicts scatter plots of the modified DFR* vs. D_m obtained from measured DSD at the values of γ of 0 and 0.5. The modified DFR* depends not only on D_m but on N_W.

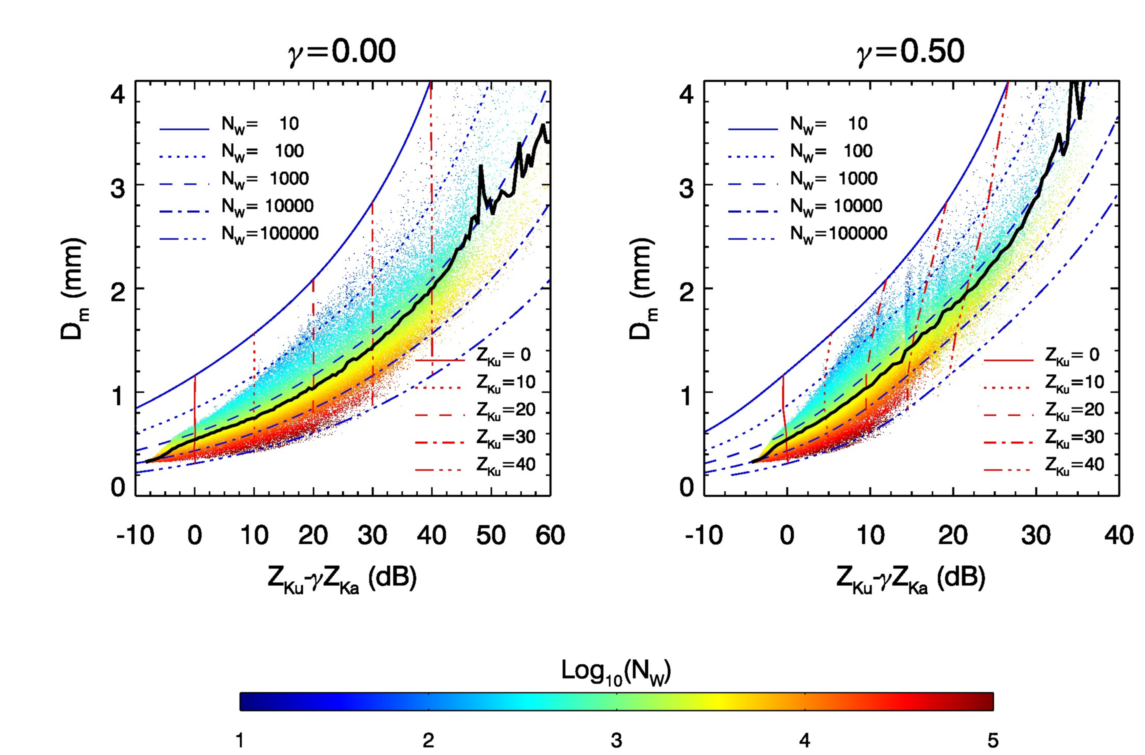

Fig.3 Scatter plots of modified DFR* vs. D_m computed from measured DSD for the values of γ of 0 (left) and 0.5 (right) with colors representing logarithm of N_W. Theoretical computations are superimposed on the plots under an assumption of gamma DSD model with a fixed μ of 3 as N_W is taken at several values. Contours of Ku-band reflectivities are also plotted.

Results & Remarks

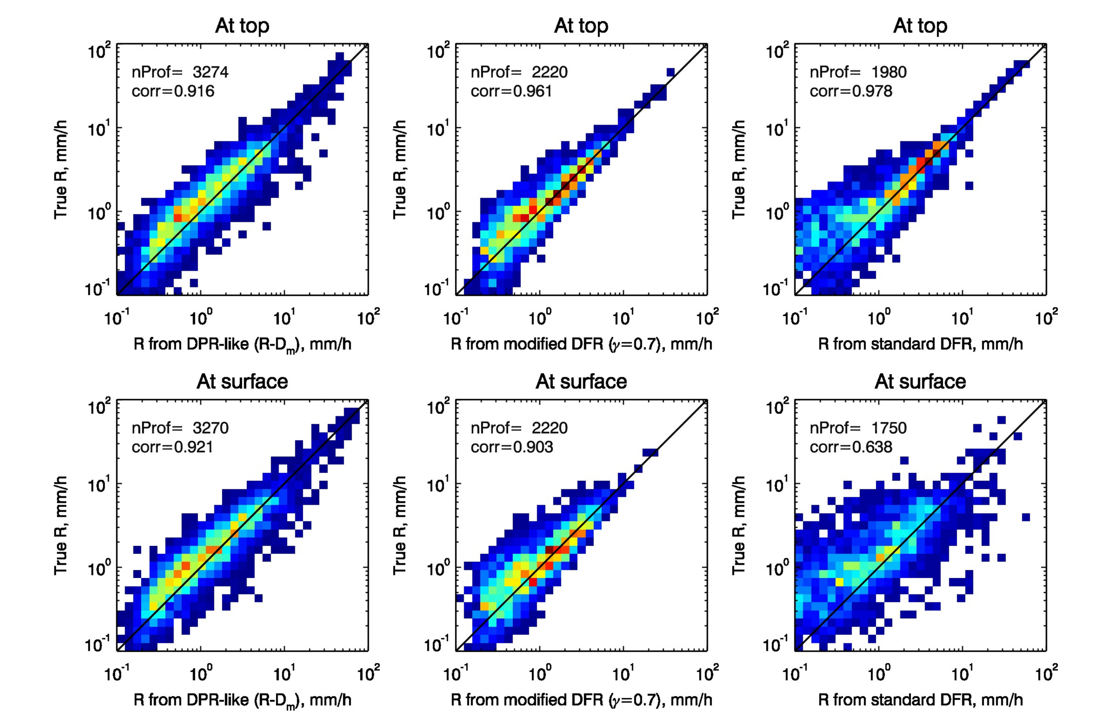

Fig.4 PDF of comparisons of rain rate between DSD derived (true) and radar retrieved results at storm top and surface as non-uniformly vertical rain profiles are simulated (as shown in the middle panels of Fig.1). The DPR-like (left), modified DFR (middle) and standard DFR (right) are included in these comparisons. Errors of the PIA and δPIA are modeled as Gaussian distribution with zero mean and standard deviations of 2 dB for PIA and 0.8 dB for δPIA.

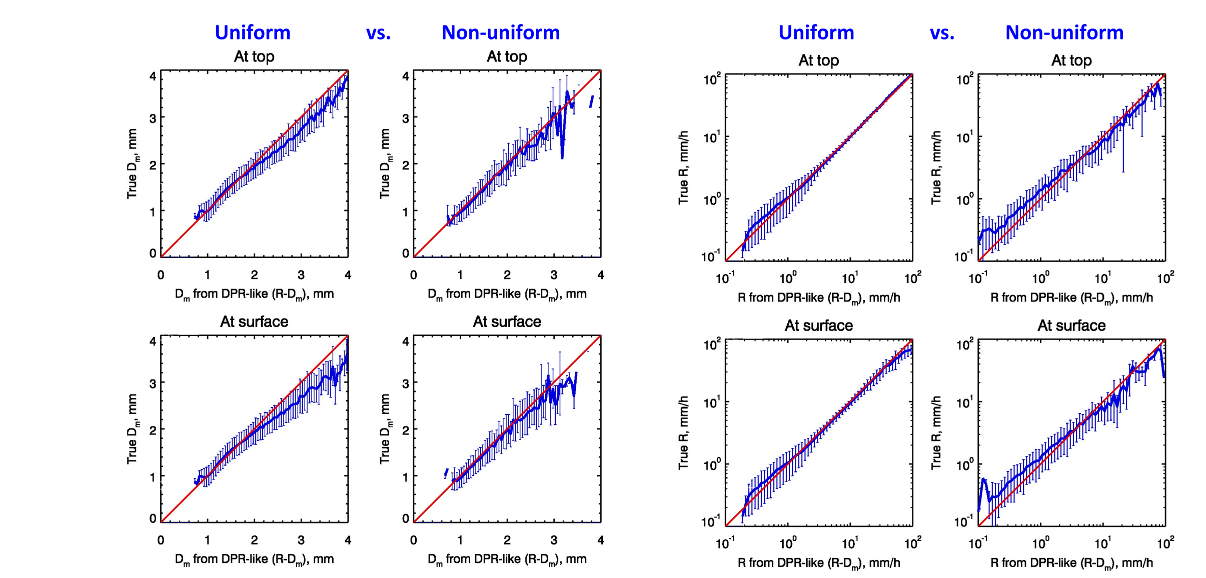

Fig.5 Comparisons of the means of dual-λ DPR-like retrieved D_m (left two columns) and rain (right two columns) with DSD-derived true values as vertical DSD profiles are assumed uniform and non-uniform. Same surface model as described in Fig.4 is used.

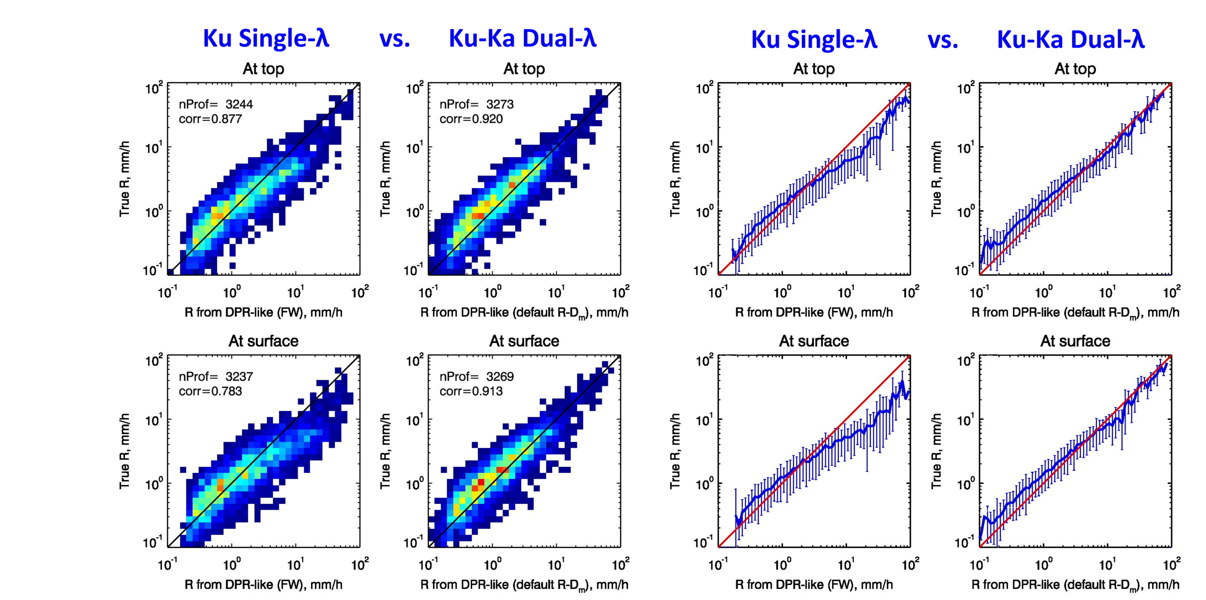

Fig.6 Comparisons of the PDF (left two columns) and means and standard deviations (right two columns) of rain retrieved by DPR-like single- and dual-wavelength algorithms. Non-uniform DSD profiles are assumed, and same surface model as described in Fig.4 is used.

Remarks

- Majority of DSD data are in the range where DFR is close to or less than zero; it leads to large uncertainties in estimates of DSD parameters and rain if the standard dual-wavelength technique (DFR) is used.
- R and DSD retrievals are improved if the modified DFR* is implemented.
- Comparisons of DSD and rain retrievals under various simulated errors and assumed vertical DSD profiles, show that DPR-like algorithms generally perform fairly well (in both robustness and accuracy).
- Dual-λ algorithms outperforms single-λ algorithms in estimates of rain in achieving better accuracy and less uncertainties.